

Microwave-hydrothermal preparation of flower-like ZnO microstructure and its photocatalytic activity

WU Shui-sheng^{1,2}, JIA Qing-ming¹, SUN Yan-lin¹, SHAN Shao-yun¹, JIANG Li-hong¹, WANG Ya-ming¹

1. Faculty of Chemical Engineering, Kunming University of Science and Technology, Kunming 650504, China;

2. Faculty of Environmental Science and Technology, Kunming University of Science and Technology, Kunming 650504, China

Received 9 July 2012; accepted 1 August 2012

Abstract: The flower-like ZnO microstructure was prepared by a straightforward microwave-hydrothermal technique using zinc chloride and arginine solution as reactants. The as-synthesized crystal structure and morphology were characterized by X-ray diffraction (XRD), scanning electron microscopy (SEM) and the optical properties of the ZnO nanostructure were studied by Raman and photoluminescence (PL) spectra, which confirms the high crystal quality of ZnO microstructure. The as-synthesized ZnO flowers exhibit a significant enhancement of photocatalytic capability toward degrading methyl blue (MB) under UV light, the photodegradation of MB reaches 95.60%, only within 2 h of adding the as-synthesized ZnO in the MB solution under UV irradiation. Furthermore, the photodegradation could be described as the pseudo-first-order kinetics with degradation rate constant of $1.0675\text{--}1.6275\text{ h}^{-1}$, which is relative to the morphology of the structures.

Key words: ZnO microstructure; microwave-hydrothermal method; photoluminescence; photodegradation

1 Introduction

Zinc oxide (ZnO) is an important semiconductor material with a wide band gap of 3.37 eV as well as a large exciton binding energy of 60 meV at room temperature, which has aroused a great interest in studying ZnO nanostructures. ZnO nanocrystal has found numerous applications, such as gas sensors [1], transparent electrodes [2], pH sensors [3], biosensors [4], acoustic wave devices [5], UV photodetector [6] and photocatalyst [7,8]. Recently, microcrystalline ZnO has been deeply researched, including single-crystalline star-shaped ZnO microcrystals with six arms [9], ZnO microcrystals with anti-Stokes photoluminescence properties [10], mushroom-like ZnO microcrystals synthesized via a solution calcinations process [11], ZnO microcrystals formed by laser irradiation method [12], and ZnO microballs synthesized by pyrolysis of zinc-acetate in oxygen atmosphere [13].

Microwave-hydrothermal reaction has been used as an effective method for the synthesis of nanoparticles

of various oxides [14–16]. Compared with conventional methods, microwave-hydrothermal synthesis has many distinct advantages, such as rapid heating to crystallization temperature, accelerating chemical reaction rate, enhancing crystallinity and decreasing byproduct. Furthermore, it is simple, energy efficient and economical. In this work, we report a microwave-hydrothermal method to generate flower-like ZnO nanostructure and investigate their optical properties and photocatalytic activity.

2 Experimental

2.1 Synthesis

The synthesis of ZnO flowers was carried out via microwave-hydrothermal method. In a typical procedure, 2 mmol of ZnCl₂ and 2 mmol of arginine were added to a stirred deionized water of 20 mL while stirring for 10 min at room temperature, correspondingly. Then arginine solution was added dropwise to ZnCl₂ solution in turn. After being vigorously stirred for 30 min at room temperature, the final clear solution was transferred to a

Teflon vessel of the MDS-6 (Microwave Digestion/Extraction System, Shanghai Sineo Microwave Chemical Technology Co. Ltd.). A temperature program was established to make the desired reaction temperature (120, 150 and 180 °C, which were denoted as ZnO-1, ZnO-2, ZnO-3) attain within about 3 min. The treatment was extended at the selected temperatures for 10 min under autogenous pressure. The as-prepared powders were repeatedly washed with the distilled water and ethanol several times, filtered and dried in an oven at 60 °C.

2.2 Characterization

The phase of as-synthesized sample was studied by X-ray diffraction (XRD) with a Bruker D8 Advance diffractometer using Cu K α radiation ($\lambda=1.54056$ Å) and operating at 40 kV and 40 mA. The morphology of as-prepared sample was examined by scanning electron microscopy (SEM, KYKY-2000), as well as Raman spectrum (Renishaw, RM 1000) measured with an excitation from the 514 nm line of an Ar-ion laser using a power of 4.7 mW. The photoluminescence property of as-synthesized sample was studied using a fluorescence spectrophotometer (JASCO FP-6500) at room temperature.

2.3 Photocatalytic activity test

The photocatalytic activity of the as-synthesized ZnO was evaluated in terms of the degradation of MB in an aqueous solution. A 250 W high-pressure mercury lamp (dominant wavelength: 365 nm) used as a UV light, was positioned inside a cylindrical vessel and surrounded by circulating water jacket for cooling. 50 mg of sample was suspended in 50 mL of an aqueous solution of 10 mg/L MB. The solution was continuously stirred at room temperature for about 30 min to ensure the establishment of an adsorption-desorption equilibrium among the photocatalyst, MB, and water before irradiation with UV light from the high-pressure mercury lamp. The distance between the light source and the bottom of the solution was about 10 cm. The concentration of MB was monitored by using a UV-vis spectrometer (Shanghai Meipuda Instrument Co. Ltd. UV-1600).

3 Results and discussion

Figure 1 presents the XRD pattern of the as-synthesized sample ZnO-3. This XRD pattern can demonstrate clearly that the product is crystalline, and the diffraction peaks can be indexed unambiguously to the wurtzite-type ZnO with lattice constants $a=3.249$ Å and $c=5.208$ Å, consistent well with the standard PDF database (JCPDS file 36-1451) [17]. The characteristic peaks are higher in intensity and narrower in spectral

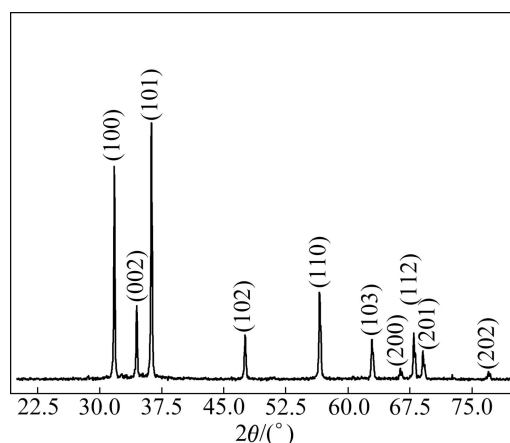


Fig. 1 XRD pattern of as-synthesized sample

width, indicating that the products are of good crystallinity. No other peaks corresponding to impurities are detected, showing that the final products purely consist of ZnO.

ZnO is a wurtzite-type structure and belongs to the space group of C_{6v}^4 [18,19] with four atoms per unit cell generating nine optical and three acoustic phonon branches [20]. We all know that the phonon modes of a crystal are subdivided into two general categories: acoustic or optical mode, transverse or longitudinal mode. According to group theory, the single crystal ZnO owns optical phonon modes including both Raman- and infrared- active A_1 and E_1 modes, only Raman-active E_2 modes, and Raman-inactive B_1 modes [21]. The A_1 and E_1 modes are polar which can be observed to split into transverse optical (TO) and longitudinal optical (LO) phonon components. Raman spectroscopy is a fast and nondestructive tool to evaluate the quality of crystalline materials, including surface conditions and homogeneity, which is very sensitive to the lattice microstructure. So, the microstructure of the ZnO microcrystals was further studied by Raman scattering technique at room temperature (Fig. 2). Raman spectrum shows all characteristic bands of crystalline ZnO at 334, 383, 410, 438, 574, and 665 cm^{-1} in the range of 200–800 cm^{-1} . The Raman peaks at 334 and 665 cm^{-1} are attributed to the second- and fourth-order overtones, i.e., $2A_1$ and $4A_1$ modes, respectively [18], which are caused by the multiphonon processes [22]. The strong Raman peak at 437 cm^{-1} is the typical characteristics of wurtzite-type of ZnO which is attributed to the nonpolar optical phonon in E_2 mode of the ZnO [18,22]. The weak Raman peak at 380 cm^{-1} is attributed to transverse optical A_1 mode, i.e., A_{1T} or $A_1(\text{TO})$ mode. The much suppressed peak at 410 cm^{-1} is attributed to transverse optical E_1 mode, i.e., E_{1T} or $E_1(\text{TO})$ mode. Both the $A_1(\text{TO})$ and $E_1(\text{TO})$ modes reflect the strength of the polar lattice bonds [23].

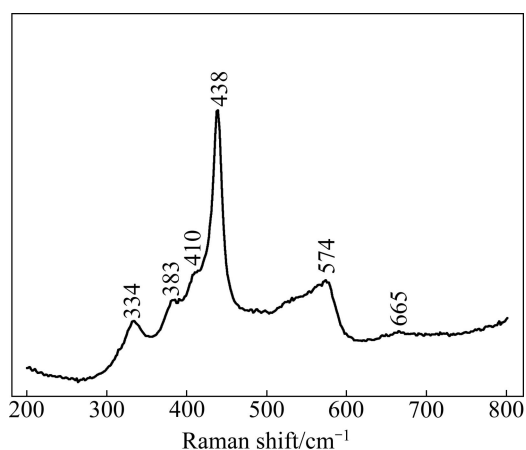


Fig. 2 Raman spectrum of as-synthesized ZnO-3 microcrystal

Figure 3 shows the SEM images of the final ZnO products synthesized at different reaction temperatures, i.e., 120, 150, 180 °C, denoted as ZnO-1, ZnO-2, ZnO-3, correspondingly. According to SEM observation, when the reaction temperature was 120 °C, ruleless rods appeared in the products with 4.5–7.0 μm in length and 0.5–1.0 μm in diameter (Fig. 3(a)), When the reaction temperature was increased to 150 °C or 180 °C, flower-like microcrystals composed of nanorods as second order compositions with diameter of 500–600 nm and 2–3.5 μm in length (Figs. 3(b) and (c)), were prepared.

Figure 4 shows the room temperature emission spectra of ZnO microcrystals dispersed in ethanol. The as-synthesized ZnO displays three PL emissions: an ultraviolet (UV) emission centered at ca. 402 nm attributed to near-band edge (NBE) emission, a violet emission at ca. 425 nm and a green emission at ca. 560 nm attributed to deep-level (DL) emission. Usually, the emission spectra can be divided into two broad categories: the NBE emission and DL emission. The UV emission at 402 nm generally originates from the direct recombination of the free excitons [19,24]. The visible emissions at 425 and 560 nm are caused by the structural defects, such as oxygen vacancies and zinc interstitials in the crystalline ZnO [25]. The 425 nm emission can be regarded as the interstitial oxygen energy level which was observed in ZnO quantum dots [26] and ZnO thin film at 420 nm [27]. This result can also be identified by the intensity reduction of Raman peak at 574 cm⁻¹ [27]. All these PL results are consistent with the Raman data and identify that the ZnO microcrystals have rather good crystal quality with fewer structural defects [19].

The photocatalytic activities of the as-synthesized ZnO microcrystals were investigated by the photocatalytic oxidation of methyl blue (MB) dye under UV irradiation (dominant wavelength: 365 nm). The characteristic absorption of MB at λ=664 nm was

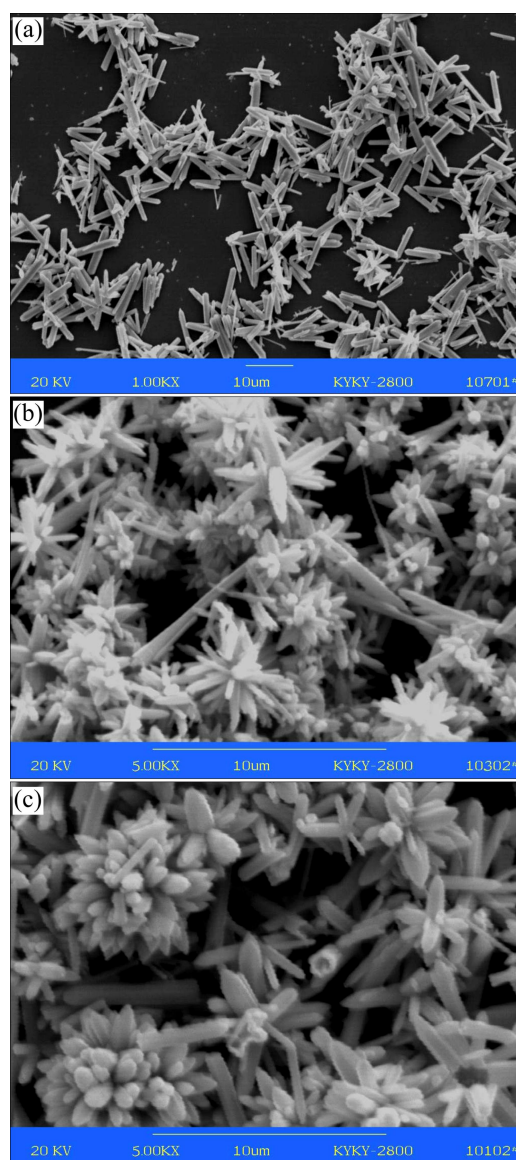


Fig. 3 SEM images of ZnO microcrystals: (a) ZnO-1; (b) ZnO-2; (c) ZnO-3

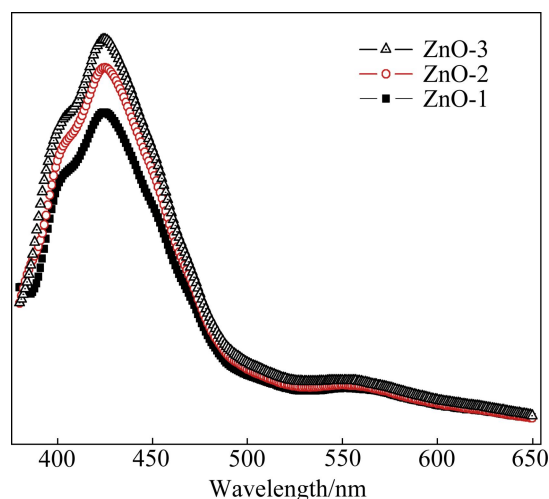


Fig. 4 PL spectra of typical as-synthesized ZnO microcrystals dispersed in ethanol excited at 345 nm

selected to monitor the photocatalytic degradation process. Figure 5(a) shows the MB concentration decreases with UV irradiation time by different ZnO samples. The blank experiment shows that the degradation of MB is less than 25% only under UV irradiation for 2 h (Fig. 5(a)). After 2 h of adding the as-synthesized ZnO-3 in the MB solution under UV irradiation, the degradation of MB reaches 95.60%, close to 100% (Fig. 5(a)). This suggests that the as-synthesized ZnO microcrystals possess intrinsic photocatalytic activity under UV irradiation. Figure 5(a) also shows that all as-synthesized ZnO microcrystals have an excellent photocatalytic performance with a degradation of MB more than 83% in 2 h. The photocatalytic activity of the as-synthesized ZnO microcrystals indicates that the ZnO microcrystals can find an excellent application in environmental protection.

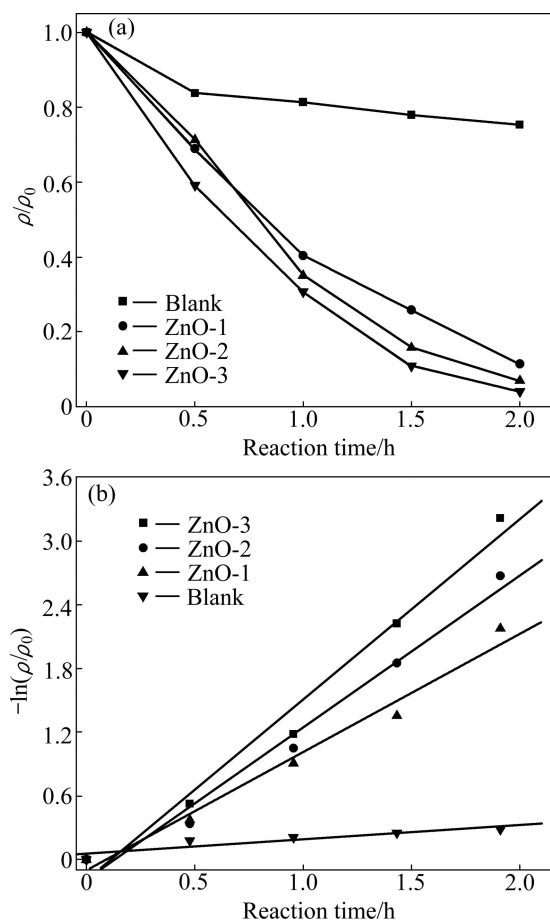


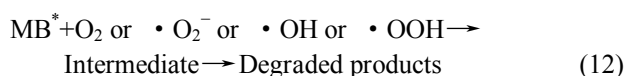
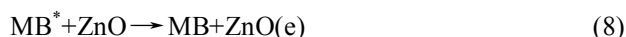
Fig. 5 Plots of photocatalytic degradation of MB concentration vs irradiation time in the presence of ZnO samples under UV light irradiation (a) and dependence of $-\ln(\rho/\rho_0)$ on irradiation time under UV light irradiation (b)

To further understand the reaction kinetics of MB degradation, the apparent pseudo-first-order model [28] expressed by Eq. (1) was applied as:

$$-\ln(\rho/\rho_0)=kt \quad (1)$$

where k is the apparent pseudo-first-order rate constant, ρ is the MB concentration in aqueous solution at time t , and ρ_0 is the initial MB concentration. Figure 5(b) shows the first-order linear fit from the experimental data, the k values of ZnO-3, ZnO-2, ZnO-1 and blank were obtained at the degradation rate of 1.6275 h^{-1} ($R^2=0.99$), 1.3721 h^{-1} ($R^2=0.98$), 1.0675 h^{-1} ($R^2=0.99$) and 0.1278 h^{-1} ($R^2=0.97$). The result shows that the flower-like microcrystal ZnO is a much more effective photocatalyst than ZnO rods.

The degradation mechanism of MB by ZnO microcrystals under UV was discussed. The possible reaction mechanism of photodegradation MB under UV light irradiation can be illustrated as follows [28,29]:



where MB, MB^* , and MB^+ represent MB molecules in the ground, excited, and oxidized states, respectively. An electron (e) is excited from the valance band into the conduction band, generating a hole (h^+) when a photon with an energy of $h\nu$ matches or exceeds the bandgap energy, E_g , of the semiconductor ZnO. First, MB is excited to its excited state (MB^*) by UV light irradiation. The excited state of MB injects electrons into ZnO microcrystals to generate the dye radical cation ($\text{MB}^{+\cdot}$). In MB solution, the OH^- reacts with h^+ and generates $\cdot\text{OH}$, i.e., $\text{OH}^-+\text{h}^+\rightarrow\cdot\text{OH}$, while O_2 can react with e and generates $\cdot\text{O}_2^-$, furthermore, the $\cdot\text{O}_2^-$ reacts with H^+ and generates $\cdot\text{OOH}$. The $\cdot\text{OOH}$, $\cdot\text{OH}$, or $\cdot\text{O}_2^-$ radical is the oxidation agent, which oxidizes organic compounds, in other words, this is favorable for the MB degradation from Eq. (12). Subsequent reactions between $\text{MB}^{+\cdot}$ (or MB) and active oxygen radicals ($\cdot\text{OOH}$, $\cdot\text{OH}$, $\cdot\text{O}_2^-$) lead to the destruction of the dye chromophore and also result in the formation of even smaller decomposed fragments after a series of complex oxidative steps.

4 Conclusions

1) The rods and flower-like ZnO microcrystals were synthesized via microwave-hydrothermal technique.

2) The Raman and PL data indicate that the ZnO microcrystals have a higher crystal quality due to the fact that the crystal growth is under thermodynamic control. The UV-emission at 402 nm is attributed to NBE emission while the visible emissions at 425 and 560 nm to DL emission. The strong UV-emission at room temperature suggests that the ZnO microcrystals may find use in optoelectronic devices in the future.

3) The as-synthesized ZnO microcrystals exhibit an excellent photocatalytic activity toward degrading methyl blue under UV light, suggesting that the ZnO microcrystals have an excellent application in environmental protection.

References

- [1] RAO B B. Zinc oxide ceramic semi-conductor gas sensor for ethanol vapour [J]. *Materials Chemistry and Physics*, 2000, 64(1): 62–65.
- [2] HORSTHUIS W H G. ZnO processing for integrated optic sensors [J]. *Thin Solid Films*, 1986, 137(2): 185–192.
- [3] ASIF M H, NUR O, WILLANDER M, DANIELSSON B. Selective calcium ion detection with functionalized ZnO nanorods-extended gate MOSFET [J]. *Biosensors and Bioelectronics*, 2009, 24(11): 3379–3382.
- [4] CAO X, NING W, LI L D, GUO L. Synthesis and characterization of waxberry-like microstructures ZnO for biosensors [J]. *Sensors and Actuators B: Chemical*, 2008, 129(1): 268–273.
- [5] KRISHNAMOORTHY S, ILIADIS A A. Development of high frequency ZnO/SiO₂/Si Devices mode surface acoustic wave devices [J]. *Solid-State Electronics*, 2006, 50(6): 1113–1118.
- [6] LUO L, ZHANG Y F, MAO S S, LIN L W. Fabrication and characterization of ZnO film based UV photodetector [J]. *Journal of Materials Science: Materials in Electronics*, 2009, 20(3): 197–201.
- [7] JIA Zhi-gang, PENG Kuan-kuan, LI Yan-hua, ZHU Rong-sun. Preparation and photocatalytic performance of porous ZnO microrods loaded with Ag [J]. *Transactions of Nonferrous Metals Society of China*, 2012, 22(4): 873–878.
- [8] ZHANG Bai-yu, HUANG Guo-he, LIU Miao, DONG De-ming, CHEN Bing, CHRISTINE W C. ZnO-based solar photocatalysis for treatment of Cr(VI) contamination [J]. *Transactions of Nonferrous Metals Society of China*, 2004, 14(1): 49–53.
- [9] LV Y Z, LI C P, GUO L, WANG Q X, WANG R M, XU H B, YANG S H, AI X C, ZHANG J P. Nanostructured stars of ZnO microcrystals with intense stimulated emission [J]. *Applied Physics Letters*, 2005, 87: 163103.
- [10] CAO W T, DU W M, SU F H, LU G H. Anti-Stokes photoluminescence in ZnO microcrystal [J]. *Applied Physics Letters*, 2006, 89: 031902.
- [11] NIU H X, YANG Q, YU F, TANG K B, XIE Y. Formation of mushroom-like ZnO microcrystals through a solution calcination process [J]. *Materials Letters*, 2007, 61(1): 137–140.
- [12] CAO W, DU W. Strong exciton emission from ZnO microcrystal formed by continuous 532 nm laser irradiation [J]. *Journal of Luminescence*, 2007, 124(2): 260–264.
- [13] XIA X H, ZHU L P, YE Z Z, YUAN G D, ZHAO B H, QIAN Q. Novel ZnO microballs synthesized via pyrolysis of zinc-acetate in oxygen atmosphere [J]. *Journal of Crystal Growth*, 2005, 282(3–4): 506–512.
- [14] KHOLLAM Y B, DESHPANDE S B, KHANNA P K, JOY P A, POTDAR H S. Microwave-accelerated hydrothermal synthesis of blue white phosphor: Sr₂CeO₄ [J]. *Materials Letters*, 2004, 58(20): 2521–2524.
- [15] LIU S F, ABOTHU I R, KOMARNENI S. Barium titanate ceramics prepared from conventional and microwave hydrothermal powders [J]. *Materials Letters*, 1999, 38(5): 344–350.
- [16] CORRADI A B, BONDIOLI F, FERRARI A M, MANFREDINI T. Synthesis and characterization of nanosized ceria powders by microwave-hydrothermal method [J]. *Materials Research Bulletin* 2006, 41: 38–44.
- [17] ZHU Jian-yu, ZHANG Jing-xia, ZHOU Hui-fen, QIN Wen-qing, CHAI Li-yuan, HU Yue-hua. Microwave-assisted synthesis and characterization of ZnO-nanorod arrays [J]. *Transactions of Nonferrous Metals Society of China*, 2009, 19(6): 1578–1582
- [18] GAO S Y, ZHANG H J, WANG X M, DENG R P, SUN D H, ZHENG G L. ZnO-based hollow microspheres: Biopolymer-assisted assemblies from ZnO nanorods [J]. *The Journal of Physical Chemistry B*, 2006, 110(32): 15847–15852.
- [19] UMAR A, HAHN Y B. ZnO nanosheet networks and hexagonal nanodiscs grown on silicon substrate: Growth mechanism and structural and optical properties [J]. *Nanotechnology*, 2006, 17: 2174–2180.
- [20] DAMEN T C, PORTO S P S, TELL B. Raman effect in zinc oxide [J]. *Physical Review*, 1966, 142: 570–574.
- [21] GUO X D, LI R X, HANG Y, XU Z Z, YU B K, MA H L, SUN X W. Raman spectroscopy and luminescent properties of ZnO nanostructures fabricated by femtosecond laser pulses [J]. *Materials Letters*, 2007, 61(23–24): 4583–4586.
- [22] WAITZ T, TIEMANN M, KLAR P J, SANN J, STEHR J, MEYER B K. Crystalline ZnO with an enhanced surface area obtained by nanocasting [J]. *Applied Physics Letters*, 2007, 90: 123108.
- [23] ASHKENOV N, MBENKUM B N, BUNDESMANN C, RIEDE V, LORENZ M, SPEMANN D, KAIDASHEV E M, KASIC A, SCHUBERT M, GRUNDMANN M, WAGNER G, NEUMANN H, DARAKCHIEVA V, ARWIN H, MONEMAR B. Infrared dielectric functions and phonon modes of high-quality ZnO films [J]. *Journal of Applied Physics*, 2003, 93: 126–133.
- [24] KONG Y C, YU D P, ZHANG B, FANG W, FENG S Q. Ultraviolet-emitting ZnO nanowires synthesized by a physical vapor deposition approach [J]. *Applied Physics Letters*, 2001, 78: 407–409.
- [25] BAGNALL D M, CHENY F, SHEN M Y, ZHU Z, GOTO T, YAO T. Room temperature excitonic stimulated emission from zinc oxide epilayers grown by plasma-assisted MBE [J]. *Journal of Crystal Growth*, 1998, 184–185: 605–609.
- [26] MAHAMUNI S, BORGHAIN K, BENDRE B S, LEPPERT V J, RISBUD S H. Spectroscopic characterization of electrochemically grown ZnO quantum dots [J]. *Journal of Applied Physics*, 1999, 85: 2861–2865.
- [27] XU X L, LAU S P, CHEN J S, CHEN G Y, TAY B K. Polycrystalline ZnO thin films on Si (100) deposited by filtered cathodic vacuum arc [J]. *Journal of Crystal Growth*, 2001, 223(1–2): 201–205.
- [28] YANG L Y, DONG S Y, SUN J H, FENG J L, WU Q H, SUN S P.

Microwave-assisted preparation, characterization and photocatalytic properties of a dumbbell-shaped ZnO photocatalyst [J]. Journal of Hazardous Materials, 2010, 179(1–3): 438–443.

[29] LI B X, WANG Y F. Facile synthesis and enhanced photocatalytic performance of flower-like ZnO hierarchical microstructures [J]. The Journal of Physical Chemistry C, 2010, 114(2): 890–896.

微波水热法合成花状纳米 ZnO 及其光催化活性

伍水生^{1,2}, 贾庆明¹, 孙彦林¹, 陕绍云¹, 蒋丽红¹, 王亚明¹

1. 昆明理工大学 化学工程学院, 昆明 650504; 2. 昆明理工大学 环境科学与工程学院, 昆明 650504

摘 要: 使用氯化锌和精氨酸作为反应物, 通过简单的微波水热技术制备花状纳米氧化锌。利用 X 射线衍射(XRD)和扫描电镜(SEM)对所合成的纳米氧化锌进行晶体结构和形貌的表征。通过拉曼光谱和光致发光(PL)光谱对纳米氧化锌的光学性能进行研究, 证实了合成物为高结晶度的纳米氧化锌。在紫外光辐射下, 合成的 ZnO 光催化降解亚甲基蓝(MB)有较好的效果, 紫外光催化 2 h 后亚甲基蓝的降解率达到 95.60%。ZnO 光催化降解亚甲基蓝可以描述为一级动力学反应, 降解速率常数在 $1.0675\sim 1.6275\text{ h}^{-1}$ 的范围中, 这与所合成的 ZnO 形貌有关。

关键词: 纳米 ZnO; 微波水热法; 光致发光; 光降解

(Edited by LI Xiang-qun)